Available online at www.sciencedirect.com

ScienceDirect

Current Opinion in Structural Biology

Toward high-resolution *in situ* structural biology with cryo-electron tomography and subtomogram averaging

Florian KM Schur

Cryo-electron tomography (cryo-ET) provides unprecedented insights into the molecular constituents of biological environments. In combination with an image processing method called subtomogram averaging (STA), detailed 3D structures of biological molecules can be obtained in large, irregular macromolecular assemblies or *in situ,* without the need for purification. The contextual meta-information these methods also provide, such as a protein's location within its native environment, can then be combined with functional data. This allows the derivation of a detailed view on the physiological or pathological roles of proteins from the molecular to cellular level. Despite their tremendous potential in *in situ* structural biology, cryo-ET and STA have been restricted by methodological limitations, such as the low obtainable resolution. Exciting progress now allows one to reach unprecedented resolutions *in situ*, ranging in optimal cases beyond the nanometer barrier. Here, I review current frontiers and future challenges in routinely determining high-resolution structures in *in situ* environments using cryo-ET and STA.

Address
Institute of Science and Technology Austria, Am Campus 1, A-3400 Klosterneuburg, Austria

Corresponding author: Schur, Florian KM (florian.schur@ist.ac.at)

Current Opinion in Structural Biology 2019, **58**:1–9

This review comes from a themed issue on **CryoEM**

Edited by **Ji-Joon Song** and **Matteo Dal Peraro**

https://doi.org/10.1016/j.sbi.2019.03.018

Introduction: *in situ* structural biology

Structural biology is both a descriptive and a quantitative experimental method, as visualizing a molecule and analyzing its structural features can allow one to directly draw conclusions on its function. To achieve this most structural biology methods employ a reductionist approach via the isolation or purification of proteins from their native environment [1] in order for them to be studied after crystallization or in solution via diffraction, nuclear magnetic resonance (NMR) spectroscopy or single-particle (SPA) cryo-electron microscopy (cryo-EM) methods. These *ex situ* conditions can be potentially detrimental to a protein's function, as biological molecules may establish dynamic and unstable interactions *in situ* or adopt transient conformations that are lost upon purification. One further difficulty lies in establishing a relation between structural information obtained in isolation with the activity of proteins in a native context, which would ultimately allow one to describe their role in cellular reaction pathways. This could be best achieved by performing exploratory structural biology to first allow detection of molecules *in situ* followed by obtaining detailed 3D information. These *in situ* data could then be linked with contextual information, by visualizing the interplay of proteins with their interaction partners, their subcellular localization and distribution and whether they might form unexpected homomeric or heteromeric assemblies. Despite the undisputed ongoing success of conventional structural biology applications [2,3], these considerations highlight the tremendous potential of *in situ* high-resolution structural biology approaches to reveal the unexpected [4,5]. For consistency, in this review the term *in situ* is used for proteins or macromolecular complexes that are not extracted from their native environment, being it in cells (or organelles) or within or on the surface of purified viruses or bacteria.

DeRosier and Klug laid the foundation for *in situ* structural biology in 1968 by introducing the concept of electron tomography (ET) [6], but it took more than two decades until automated data acquisition [7] and efficient image processing software (such as Ref. [8]) allowed ET to develop into a key method in cell biology to study the organization and ultrastructure of chemically fixed and contrasted specimens. The potential of ET was significantly extended by the ability to study proteins in their native hydrated state via vitrification [9], allowing cryo-ET and subtomogram averaging (STA) to describe the unperturbed organization of reconstituted assemblies, intact viruses and frozen-hydrated cells (Figure 1). While the potential of cryo-ET and STA has been widely acknowledged [10], several methodological limitations necessitate trade-offs between experimental practicality and achievable resolution [11,12]. This has restricted cryo-ET and STA to lower resolutions compared to other structural biology techniques. To acknowledge this difference, the term high-resolution in cryo-ET is commonly used for subnanometer resolutions. Despite the mentioned limitations, recent progress in obtaining sub-5 Å resolution structures from ideal samples [13••,14•]

Figure 1

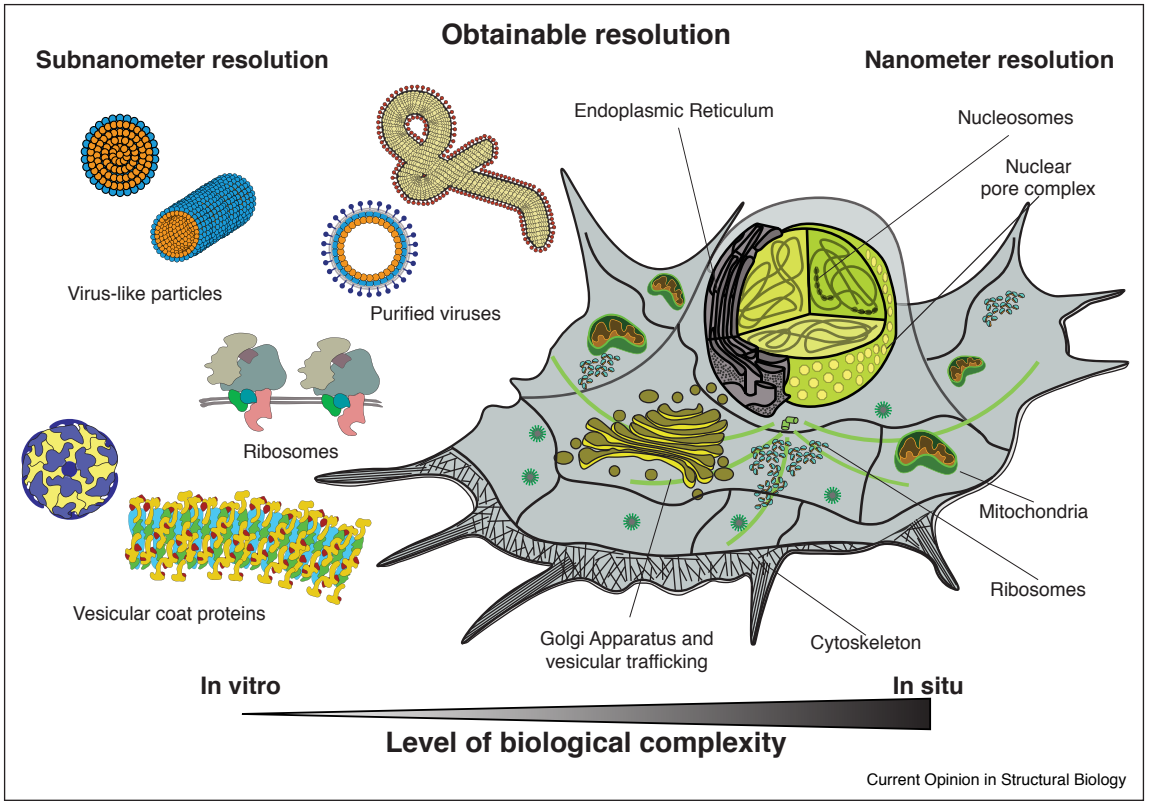

In vitro and *in situ* applications in cryo-ET and subtomogram averaging.
Cryo-ET and subtomogram averaging allow the structural analysis of specimens of varying complexity and within different environments. With an increasing level of sample complexity (such as studying proteins within cells) the biological information (including contextual information of the studied protein) can increase as well, but resolutions are lower due to higher experimental challenges. The highest resolutions have been reported for *in vitro* assembled virus-like particles, purified viruses (e.g. retroviruses and filoviruses), ribosomes and vesicular coat proteins. Cellular cryo-ET can be directly performed on peripheral regions of the cell such as cytoskeletal protrusions, but often requires additional sample preparation steps, where thin sections of the specimen are obtained, for example, with focused ion beam milling. Structures that have been visualized in cells include ribosomes, proteasomes, the nuclear pore complex, proteins of the vesicular trafficking machinery and nucleosomes. Schematic depictions of the individual specimens are not shown to scale.

shows that cryo-ET and STA can be valid high-resolution structure determination techniques.

Here, I will review current methodological frontiers and applications as well as new developments in cryo-ET and STA to highlight challenges that need to be addressed to allow these methods to routinely obtain high-resolution structures *in situ* in the future.

Basics of cryo-ET and subtomogram averaging

For excellent reviews on the basic principles of cryo-ET and STA the reader is referred to existing literature [10,15•]. In cryo-ET 3D reconstructions (so called tomograms) of biological structures are calculated from incrementally acquired projection images of the same object, separated by defined tilt angles (called a tilt series). In contrast to other cryo-EM methods, cryo-ET does not rely on the repetitive occurrence of structures for 3D reconstruction, and individual macromolecular complexes and organelles can be described to a resolution of several nanometres. When many copies of a structure exist within a tomogram, STA can be applied. Here the reconstructions of the individual copies are iteratively aligned and averaged, ultimately leading to a higher signal-to-noise ratio (SNR) and higher-resolution details. STA is particularly successful when applied to specimens that display local or global symmetry, a rigid conformation, electron-dense regions (e.g. ribonucleic acids) or provide a-priori information on orientational parameters [15•]. Such samples, most notably viruses, have been useful tools to develop new methods in EM, and naturally have also contributed significantly to advances in cryo-ET and STA [16,17] (Figures 1 and 2).

Overcoming the limitations

The ultimate resolution-limiting factor in imaging vitrified specimens is radiation damage caused by the

Figure 2

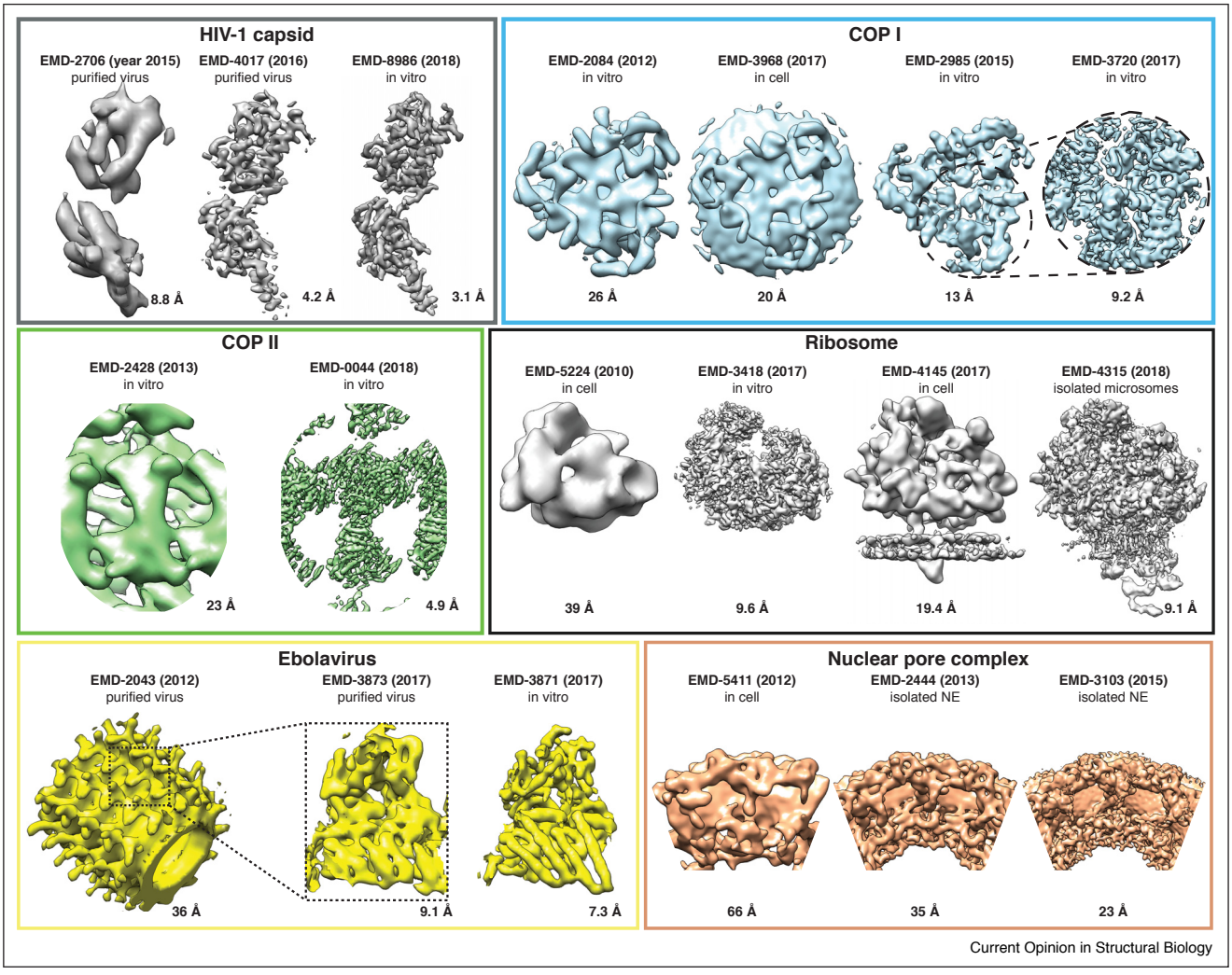

Resolutions in cryo-ET and subtomogram averaging.
This gallery highlights the diversity of samples that can be studied via cryo-ET and STA and also the increasing resolutions obtained within only a few years. Because of the significant improvement of data acquisition and image processing methods, subnanometer resolutions can now be more regularly achieved, and in selected cases resolutions beyond 5 Å are possible. *In situ* structures (from within cells, purified viruses or isolated organelles) can be obtained at resolutions that previously only were accessible to *in vitro* reconstituted specimens. For the different examples the EMDB accession number and the source of the structure is given, together with the publication year (in brackets).
Depicted structures are HIV-1 CA assemblies [13••,16,51••], COPI and COPII vesicular coat proteins [14•,68,69,78–80], ribosomes [31,64–66], Ebolavirus [56,57], and the NPC [60–62].

cumulative electron dose. This is particularly apparent in cryo-ET where the cumulative dose needs to be distributed over an entire tilt series resulting in individual projections with low SNR. According to the dose-fractionation theorem, statistically significant 3D reconstructions in ET can be obtained from individual projections with very low SNR [18]. As a 3D reconstruction in theory contains more information than one 2D-micrograph acquired with the same dose [19], cryo-ET in theory holds the promise to unify the potential of other cryo-EM imaging modalities to determine high-resolution structures of different samples such as purified or reconstituted isolated complexes or imperfect crystalline specimens [20]. Still, the low SNR of individual projections influences data acquisition and processing steps, including tilt series alignment, particle detection, and STA.

Another inherent limitation in cryo-ET is the typically increased sample thickness of the studied specimen, which leads to increased scattering of electrons and reduced image contrast. Energy-filtered transmission electron microscopy (EFTEM) is, therefore, particularly advantageous in cryo-ET, as it increases image contrast

by removing inelastically scattered electrons. In order to obtain insights into specimens that are too thick for transmission electron microscopy (TEM), such as most regions of cells, additional sample preparation steps are necessary, including focused ion beam milling scanning electron microscopy (FIB-SEM, for details, the reader is referred to Ref. [21]).

Frontiers in data acquisition

In high-resolution cryo-ET, the requirement of using high magnification, resulting in a small pixel size and hence a restricted field of view, negatively impacts the dataset size. During tilt series acquisition, the area of interest has to remain precisely centered. Mechanical movements of the stage limit the accuracy to several micrometers, but this can be compensated by fully automated data acquisition in several free [22–24] and commercial software packages (e.g. Thermo Fisher Tomography, Gatan Latitude S, TVIPS EM-Tomo). Here, undesired stage shifts are corrected via iterative tracking and focusing. Stage stability directly effects acquisition speed; this can be increased by improving stability during movement using a more eucentric single-axis specimen holder, which has been shown to allow using fast acquisition schemes without the need of tracking [25•].

When acquiring a tilt series, not all views of the sample can be obtained. This is due to the mechanical limitations of the specimen holder, which obstructs the beam at high tilts, and due to tilting the specimen in discrete angular steps. This results in the so-called missing wedge and missing information in Fourier space, causing anisotropic information in reconstructed tomograms [15•]. The effect of the missing wedge can be reduced if a second tilt series around the orthogonal axis is acquired [26]. This is not commonly done in cryo-ET, as the cumulative electron dose for such dual axis acquisition can be too destructive. With the advent of high-sensitivity direct electron detectors (DED) and, therefore, lower required dose, dual axis tomography becomes a feasible and tempting option for many structural and cell biology questions. The information retained in the second tilt series could prove to be beneficial for the optimal reconstruction of, for example, helical and filamentous specimens that are oriented perpendicularly to the tilt axis and for improving alignment accuracy in STA [26,27]. Alternatively, *in silico* approaches to restore missing wedge information during tomogram reconstruction have been proposed [28,29], but their potential for high-resolution studies still remains to be evaluated. STA itself helps to overcome the missing wedge as individual copies of particles, differently oriented with respect to the missing wedge within a tomogram, can be summed to generate an isotropic structure.

Depending on the target resolution that should be achieved, the selection of the tilt scheme (i.e. the number and sequence in which the images are acquired) will again determine a trade-off between dataset size and high-resolution content in tomograms. Maximizing high-resolution content in a tomogram can be achieved when using a dose-symmetric tilt scheme [30], which ensures the optimal distribution of dose over a tilt series, but results in smaller datasets due to the reduced acquisition speed.

Phase contrast in cryo-EM is traditionally obtained by acquiring out-of-focus micrographs, which results in the loss of high-resolution content due to the defocus-dependent contrast transfer function (CTF). Alternatively, instead of deliberately defocusing the image to gain phase contrast, so-called phase plates can be used. They modulate the electron wave by introducing a phase shift that results in improved contrast at low and high spatial frequencies. One particular implementation of such a phase plate, the Volta phase plate (VPP), has been used in combination with in-focus cryo-ET and STA to yield a structure of isolated ribosomes at 9.6 Å resolution [31], demonstrating its applicability for STA approaches. One major limitation in using phase plates for high-resolution cryo-ET is the required high focusing accuracy to ensure retention of high-resolution signal within micrographs, again restricting data acquisition speed. The VPP can also be combined with conventional defocus data acquisition to improve the low-resolution signal, facilitating further image processing and data interpretation (i.e. feature identification) when working with cellular specimens [32].

All these factors underline that cryo-ET data acquisition requires the balancing of a large number of experimental factors, which need to be properly considered in order to achieve the desired outcome.

Frontiers in image processing

High-resolution information that is lost because of defocusing can be restored via correction for the CTF, which depends on an accurate estimation of the defocus value of the acquired micrograph. CTF correction in cryo-ET suffers from an increased degree of complexity due to the defocus change across a tilted sample, the higher sample thickness and the low SNR of the individual projections. Defocus estimation in cryo-ET can be facilitated by using extended tilt schemes with additional high-dose focusing areas [33], which can yield deviating results if the sample is not planar. Alternatively, imaging at a stable eucentric height allows averaging of signal of all tilts in a series and hence boosting the SNR [34,35]. New DEDs can achieve higher SNR and most often the defocus can be more reliably estimated from individual projections, resulting in a more precise CTF-correction [13••].

In 2D-CTF correction the defocus ramp in a tilted sample is taken into account by either correcting lines or tiles with a defocus value that is dependent on the distance

from the tilt axis [35–37]. Several 3D CTF-correction methods have been proposed that also account for the defocus difference caused by the varying height of objects within a sample [38,39], but have not been widely used partially due to the high computational costs. A recently proposed, computationally efficient 3D-CTF correction algorithm [40•], compatible with one of the standard tomogram reconstruction workflows, has led to a significant increase in resolution and the ability to obtain a sub 4 Å reconstruction from considerably smaller datasets than obtained via conventional 2D-CTF correction. CTF correction can also be performed on Fourier slices of subtomograms, allowing CTF refinement and missing wedge compensation during reconstruction [17].

Before tomogram reconstruction the individual projections of a tilt series need to be precisely aligned, either via additional fiducial markers (e.g. colloidal gold) or based on features of the specimen [41,42]. *In situ* data obtained from focused ion beam milled samples mostly rely on fiducial-less alignment, although the low SNR of the individual projections can preclude their precise alignment. Alternative methods have been proposed to add gold fiducial markers post-vitrification, hence being compatible with FIB-milling experiments [43].

Structure determination is only possible when the molecules of interest can be reliably identified. To this end different reconstruction, deconvolution and denoising approaches are used to improve contrast of tomograms. The SNR in reconstructed tomograms can also be increased computationally by weighting the individual images of a tilt series for cumulative electron dose, hence accounting for dose-dependent loss of high spatial frequencies [44•]. Localizing proteins of interest in tomograms can be performed via manual or automatic segmentation or via template matching [45]. Neural Networks and Deep learning have been implemented in different fields of life sciences, including SPA cryo-EM [46]. They also offer potential for a faster and effortless analysis of complex *in situ* cryo-ET data, as recently shown with the development of a convolutional deep neural network for the automatic annotation of cellular cryo-electron tomograms [47].

STA can be performed in several software packages [17,24,48–50,51••] using either angular search, fast rotational matching or maximum-likelihood (ML) approaches. These packages require different levels of user expertise and provide either a complete framework (e.g. including data management and particle identification) or reduced functionalities for simple STA analysis.

Compared to single-particle cryo-EM, image processing in cryo-ET and STA contains an increased number of interpolations, which can further attenuate the obtainable resolution. These interpolations include the alignment of the individual projections of a tilt series before tomogram reconstruction, interpolations that can occur during the reconstruction process and finally those during STA-alignment to generate a higher-resolved structure. Hybrid approaches combining 3D and 2D refinements have been used to compensate for this increased number of interpolations in cryo-ET and STA [51••,52]. Exciting progress was very recently reported via such a hybrid approach using subtomograms as fiducial markers to iteratively refine tilt series alignment [51••]. In this work the authors benchmarked their software emClarity using the publicly available raw data of the cryo-ET dataset containing immature HIV-1 assemblies [13••]. This has allowed them to obtain the highest resolution structure in cryo-ET and STA to date.

Computational sorting (or classifying) of the different conformational states biological molecules can display is absolutely critical to obtain high resolutions, but is aggravated in cryo-ET by the low SNR and the missing wedge. Different methods using either constrained-cross correlation, multi-reference alignment, principle component analysis or ML for classification have been proposed [15•,51••,53,54].

This summary highlights the plethora of available solutions for computational processing of cryo-ET and STA data. Most current workflows include a combination of the aforementioned tools and hence require a distinct level of expertise to ensure optimal results. Future attempts will be important to unify the potential of all of these methods and to design a robust workflow that is applicable to a variety of samples. The availability of published datasets in public repositories such as the Electron microscopy public image archive (EMPIAR) will be important to enable a referenced comparison of different approaches in processing cryo-ET data, including tomogram reconstruction, classification and STA.

Applications: exploring the unknown

Cryo-ET and STA have been successful in revealing the structure and arrangement of viral proteins *in vitro* and *in situ* [13••,55–57], nuclear pore complexes (NPC) in cells or purified nuclear envelopes (NE) [58–62], ribosomes and polysomes [31,63–66], ion channel receptors [67], vesicular coat proteins [14•,68,69,70••], bacterial secretion systems, chemoreceptor arrays and S-layers [20,71,72], cytoskeletal elements (such as microtubules and associated motor proteins [73]), and the complement system [74]. For several samples, the resolution that could be achieved increased significantly over the last years (Figure 2), as a result of the continued development of experimental techniques and improved hardware. *In situ* approaches have also revealed new roles for previously extensively studied proteins such as proteasomes [75,76••], underlining the exploratory potential of cryo-ET.

Bacteria, viruses and their components

Retrovirus capsid (CA) proteins have been shown to be the ideal specimen to optimize data acquisition and image processing workflows for high-resolution cryo-ET. The large copy number of assembled retroviral CA in virus particles, inherent local symmetry, and low conformational flexibility have all contributed to the fact that retrovirus assemblies were the first to be solved to subnanometer resolutions using cryo-ET and STA [16,34]. With the use of better detectors, the implementation of the described dose-symmetric tilt scheme [30], movie-mode processing [77] and weighting of tilts for cumulative dose [44•] resolutions beyond 4 Å were achieved [13••]. This revealed important features in virus assembly and maturation.

Filoviruses such as Ebola or Marburg are the causative agents of deadly hemorrhagic fevers, and form pleomorphic enveloped helical virus particles. These particles contain multiple helical symmetries that can switch within individual viruses, imposing limitations on helical reconstruction analysis. In STA, no knowledge of helical symmetry parameters is required, as subunits within a helical assembly can be treated individually. Wan and colleagues determined the structure of recombinant Ebolavirus nucleocapsid (NC)-like particles by cryo-ET and STA to 7 Å resolution [57]. The authors then validated these structures with subnanometer resolution reconstructions of NC within intact Ebola and Marburg virus particles. This provided detailed insights into nucleoprotein oligomerization, NC condensation and how RNA and accessory proteins are recruited during virus assembly.

Bacterial S-layer proteins form a symmetric and regular layer that is part of the cell envelope of many bacteria and archaea, which provides mechanical stability and protection from the extracellular environment. *In situ* information on the structure of the S-layer has been scarce due to the increased thickness of bacterial cells and high-resolution structural information has been only available for purified components. Bharat *et al.* used cryo-ET and STA on Caulobacter crescentus to solve the structure of its intact hexameric S-layer *in situ* at 7.7 Å resolution [72]. In combination with X-ray crystallography data a pseudo-atomic model of the *in situ* S-layer was then generated, helping to explain how the surface layer can simultaneously be a permeable and tough barrier.

Intracellular transport: coated vesicles

Cargo-selective trafficking vesicles emanating from the plasma membrane, Golgi, ER or endosomal membranes are dependent on the Clathrin, COPI, COPII, or retromer complex protein coats, respectively. Single-particle reconstruction methods revealed cage structures for COPII and clathrin-coated vesicles but were not able to address the entire geometric complexity of these coated vesicles. Using cryo-ET and STA the ***COPI coat*** in *in situ* and *in vitro* assembled vesicles was solved at increasing resolutions in a series of publications [68,78,79], with a recent subnanometer description of the coat structure [69]. Similarly, cryo-ET and STA were used to describe the structure of the ***retromer*** coat assembled *in vitro* on membrane tubules to ~9 Å resolution, revealing a new coat architecture [70••]. Again, in combination with *in situ* analysis this structure provided insights into coat assembly mechanisms and revealed conserved functions to induce membrane bending and cargo-binding among COPI and retromer.

Recently, the structure of the ***COPII coat*** was determined to 4.9 Å exploiting novel developments in hardware and software [14•]. This represents a significant improvement to the 23 Å structure determined only a few years earlier [80]. Such a tremendous progress highlights the fast-paced development in cryo-ET and STA methods, but also clearly displays the current limitation that for resolutions beyond 5 Å well-ordered specimens are necessary.

The nucleus and its periphery

Nucleosomes, the organizers of chromatin, are small complexes of only about 200 kDa in size, whose detection in *in situ* cryo-ET data represents a considerable challenge. Using an *in silico* purification approach Cai *et al.* [81] were able to detect nucleosomes within the nucleus of HeLa cells. STA then determined structures of nucleosome cores and mapped their positions back into euchromatic and heterochromatic regions within the nucleus, suggesting irregular paths of sequential nucleosomes.

The enormous dimensions of the ***nuclear pore complex*** represent a significant challenge to structural determination approaches. Within the last years a dramatic gain in the structural understanding of the NPC from different species was achieved by cryo-ET and STA [58] and parts of the structure of human and frog NPCs within the nuclear envelope (NE) are now determined to ~20 Å [82,83]. Despite this progress, NPCs remain an experimental challenge due to their non-perfect circularity and the relatively small datasets that usually can be obtained.

Cryo-ET and STA described novel roles for ***proteasomes***. It was found that proteasomes can bind at two distinct sites of the NPC, where they would be able to perform quality control of proteins shuttling in and out of the nucleus [75]. In another experiment, cryo-ET and subtomogram averaging showed the sequestration of proteasomes in neurodegenerative disease models, providing an explanation for the reduced degradation of protein aggregates in these pathological conditions [76••]. In all of these cases, despite the considerably low resolutions obtained, specific functional states that could only be observed *in situ* could be assigned to the proteins.

Conclusions

Development in single-particle cryo-EM has been driven by optimal test specimens, and this method can now provide near-atomic resolution structures from diverse and challenging samples. It is fair to assume that with further methodological advancements cryo-ET and STA can undergo the same development in the future.

Alongside potential improvements in image processing (such as more robust CTF determination algorithms for low SNR projections) there is also potential in hardware based improvements, for example more stable piezo-driven stages [84], allowing faster acquisitions resulting in larger datasets. In this context, it is tempting to consider a complete redesign of specimen grids to restrict undesired movements during data acquisition. New DEDs with significantly larger chip sizes are now available. This will help to increase the data throughput, but requires the development of more efficient image processing algorithms and workflows that can deal with the increasing amount of data. Pushing the boundaries of cryo-EM can be an iterative process. In the context of cryo-ET this implies repeated access to TEMs to ensure continuous improvement of acquisition conditions. Despite the exciting development of SPA cryo-EM, where sub-3 Å structures can be obtained on mid-range 200 keV microscopes [85], this will remain a challenge for cryo-ET as the increased sample thickness might require access to high-voltage microscopes with energy-filtered DEDs.

Despite the promising progress in cryo-ET and STA, for many challenging specimens integrative structural biology approaches will remain vital, for example using high-resolution a priori information obtained either by diffraction or NMR methods. There is still a long way to go until high resolutions *in situ* can be routinely achieved, but in the meantime cryo-ET and STA will continue to reveal exciting and uncharacterized structures as they have done in the past.

Conflict of interest statement

Nothing declared.

Acknowledgements

I thank William Wan for critical reading of the manuscript, and Wim Hagen and Carrie Bernecky for helpful discussions. I apologize to authors of primary literature and outstanding research using cryo-ET and subtomogram averaging that I could not cite here due to space restraints. The author acknowledges support from IST Austria and the Austrian Science Fund (FWF).

References and recommended reading

Papers of particular interest, published within the period of review, have been highlighted as:

- • of special interest
- •• of outstanding interest

1. Asano S, Engel BD, Baumeister W: **In situ cryo-electron tomography: a post-reductionist approach to structural biology**. *J Mol Biol* 2016, **428**:332-343.

2. Shi Y: **A glimpse of structural biology through X-ray crystallography**. *Cell* 2014, **159**:995-1014.

3. Fernandez-Leiro R, Scheres SHW: **Unravelling biological macromolecules with cryo-electron microscopy**. *Nature* 2016, **537**:339-346.

4. Engel BD, Schaffer M, Albert S, Asano S, Plitzko JM, Baumeister W: **In situ structural analysis of Golgi intracisternal protein arrays**. *Proc Natl Acad Sci U S A* 2015, **112**:11264-11269.

5. Dobro MJ, Oikonomou CM, Piper A, Cohen J, Guo K, Jensen T, Tadayon J, Donermeyer J, Park Y, Solis BA *et al.*: **Uncharacterized bacterial structures revealed by electron cryotomography**. *J Bacteriol* 2017, **199**:e00100-17.

6. De Rosier DJ, Klug A: **Reconstruction of three dimensional structures from electron micrographs**. *Nature* 1968, **217**:130-134.

7. Dierksen K, Typke D, Hegerl R, Koster AJ, Baumeister W: **Towards automatic electron tomography**. *Ultramicroscopy* 1992, **40**:71-87.

8. Kremer JR, Mastronarde DN, McIntosh JR: **Computer visualization of three-dimensional image data using IMOD**. *J Struct Biol* 1996, **116**:71-76.

9. Dubochet J, Adrian M, Chang JJ, Homo JC, Lepault J, McDowall AW, Schultz P: **Cryo-electron microscopy of vitrified specimens**. *Q Rev Biophys* 1988, **21**.

10. Briggs JA: **Structural biology in situ–the potential of subtomogram averaging**. *Curr Opin Struct Biol* 2013, **23**:261-267.

11. Voortman LM, Vulović M, Maletta M, Voigt A, Franken EM, Simonetti A, Peters PJ, van Vliet LJ, Rieger B: **Quantifying resolution limiting factors in subtomogram averaged cryo-electron tomography using simulations**. *J Struct Biol* 2014, **187**:103-111.

12. Turoňová B, Marsalek L, Slusallek P: **On geometric artifacts in cryo electron tomography**. *Ultramicroscopy* 2016, **163**:48-61.

13. •• Schur FKM, Obr M, Hagen WJH, Wan W, Jakobi AJ, Kirkpatrick JM, Sachse C, Kräusslich HG, Briggs JAG: **An atomic model of HIV-1 capsid-SP1 reveals structures regulating assembly and maturation**. *Science (80-)* 2016, **353**:506-508.
This study reported the first sub 4 Å resolution structure obtained by cryo-ET and subtomogram averaging, using an optimized data acquisition and image processing workflow. This proved the applicability of these methods for high-resolution studies.

14. • Hutchings J, Stancheva V, Miller EA, Zanetti G: **Subtomogram averaging of COPII assemblies reveals how coat organization dictates membrane shape**. *Nat Commun* 2018, **9**:4154.
This work reports the so far only second specimen to reach sub-5 Angstrom resolutions in cryo-ET and subtomogram averaging. Optimally chosen data acquisition conditions and image processing yielded a structure of the *in vitro* assembled COPII coat at 4.9 Å.

15. • Wan W, Briggs JAG: **Chapter thirteen - cryo-electron tomography and subtomogram averaging**. In *Methods in Enzymology*. Edited by Crowther RA. Academic Press; 2016:329-367.
This chapter provides an exhaustive overview on the cryo-ET and subtomogram averaging workflow. It summarizes important practical and theoretical aspects of data acquisition and image processing, alongside novel developments.

16. Schur FKM, Hagen WJH, Rumlová M, Ruml T, Müller B, Kraüsslich HG, Briggs JAG: **Structure of the immature HIV-1 capsid in intact virus particles at 8.8 Å resolution**. *Nature* 2015, **517**:505-508.

17. Bharat TAM, Russo CJ, Löwe J, Passmore LA, Scheres SHW: **Advances in single-particle electron cryomicroscopy structure determination applied to sub-tomogram averaging**. *Structure* 2015, **23**:1743-1753.

18. Hegerl R, Hoppe W: **Influence of electron noise on three-dimensional image reconstruction**. *Z Naturforsch A* 1976, **31**:1717.

19. McEwen BF, Downing KH, Glaeser RM: **The relevance of dose-fractionation in tomography of radiation-sensitive specimens**. *Ultramicroscopy* 1995, **60**:357-373.

20. Cassidy CK, Himes BA, Alvarez FJ, Ma J, Zhao G, Perilla JR, Schulten K, Zhang P: **CryoEM and computer simulations reveal a novel kinase conformational switch in bacterial chemotaxis signaling**. *eLife* 2015, **4**.

21. Villa E, Schaffer M, Plitzko JM, Baumeister W: **Opening windows into the cell: focused-ion-beam milling for cryo-electron tomography**. *Curr Opin Struct Biol* 2013, **23**:771-777.

22. Mastronarde DN: **Automated electron microscope tomography using robust prediction of specimen movements**. *J Struct Biol* 2005, **152**:36-51.

23. Suloway C, Shi J, Cheng A, Pulokas J, Carragher B, Potter CS, Zheng SQ, Agard DA, Jensen GJ: **Fully automated, sequential tilt-series acquisition with Leginon**. *J Struct Biol* 2009, **167**:11-18.

24. Nickell S, Forster F, Linaroudis A, Net WD, Beck F, Hegerl R, Baumeister W, Plitzko JM: **TOM software toolbox: acquisition and analysis for electron tomography**. *J Struct Biol* 2005, **149**:227-234.

25. • Chreifi G, Chen S, Metskas LA, Kaplan M, Jensen GJ: **Rapid tilt-series acquisition for electron cryotomography**. *J Struct Biol* 2019, **205**:163-169.
The increased stability of a new single-axis specimen holder enabled the authors to develop two new acquisition methods to accelerate tilt series acquisition by eliminating tracking. This potentially allows acquiring datasets that are comparable in speed and size to what currently is only obtainable in single-particle cryo-EM.

26. Iancu CV, Wright ER, Benjamin J, Tivol WF, Dias DP, Murphy GE, Morrison RC, Heymann JB, Jensen GJ: **A "flip–flop" rotation stage for routine dual-axis electron cryotomography**. *J Struct Biol* 2005, **151**:288-297.

27. Guesdon A, Blestel S, Kervrann C, Chrétien D: **Single versus dual-axis cryo-electron tomography of microtubules assembled in vitro: limits and perspectives**. *J Struct Biol* 2013, **181**:169-178.

28. Deng Y, Chen Y, Zhang Y, Wang S, Zhang F, Sun F: **ICON: 3D reconstruction with "missing-information" restoration in biological electron tomography**. *J Struct Biol* 2016, **195**:100-112.

29. Chen Y, Förster F: **Iterative reconstruction of cryo-electron tomograms using nonuniform fast Fourier transforms**. *J Struct Biol* 2014, **185**:309-316.

30. Hagen WJH, Wan W, Briggs JAG: **Implementation of a cryo-electron tomography tilt-scheme optimized for high resolution subtomogram averaging**. *J Struct Biol* 2017, **197**:191-198.

31. Khoshouei M, Pfeffer S, Baumeister W, Förster F, Danev R: **Subtomogram analysis using the Volta phase plate**. *J Struct Biol* 2017, **197**:94-101.

32. Mahamid J, Pfeffer S, Schaffer M, Villa E, Danev R, Cuellar LK, Förster F, Hyman AA, Plitzko JM, Baumeister W: **Visualizing the molecular sociology at the HeLa cell nuclear periphery**. *Science* 2016, **351**:969-972.

33. Eibauer M, Hoffmann C, Plitzko JM, Baumeister W, Nickell S, Engelhardt H: **Unraveling the structure of membrane proteins in situ by transfer function corrected cryo-electron tomography**. *J Struct Biol* 2012, **180**:488-496.

34. Schur FKM, Hagen WJH, De Marco A, Briggs JAG: **Determination of protein structure at 8.5 Å resolution using cryo-electron tomography and sub-tomogram averaging**. *J Struct Biol* 2013, **184**:394-400.

35. Zanetti G, Riches JD, Fuller SD, Briggs JA: **Contrast transfer function correction applied to cryo-electron tomography and sub-tomogram averaging**. *J Struct Biol* 2009, **168**:305-312.

36. Xiong Q, Morphew MK, Schwartz CL, Hoenger AH, Mastronarde DN: **CTF determination and correction for low dose tomographic tilt series**. *J Struct Biol* 2009, **168**:378-387.

37. Fernandez JJ, Li S, Crowther RA: **CTF determination and correction in electron cryotomography**. *Ultramicroscopy* 2006, **106**:587-596.

38. Voortman LM, Stallinga S, Schoenmakers RH, van Vliet LJ, Rieger B: **A fast algorithm for computing and correcting the CTF for tilted, thick specimens in TEM**. *Ultramicroscopy* 2011, **111**:1029-1036.

39. Kunz M, Frangakis AS: **Three-dimensional CTF correction improves the resolution of electron tomograms**. *J Struct Biol* 2017, **197**:114-122.

40. • Turoňová B, Schur FKM, Wan W, Briggs JAG: **Efficient 3D-CTF correction for cryo-electron tomography using NovaCTF improves subtomogram averaging resolution to 3.4 Å**. *J Struct Biol* 2017, **199**:187-195.
This accurate 3D-CTF correction approach allows obtaining high resolutions from significantly smaller datasets than what was previously achievable. NovaCTF is compatible with the standard cryo-ET workflow in IMOD.

41. Noble AJ, Stagg SM: **Automated batch fiducial-less tilt-series alignment in Appion using Protomo**. *J Struct Biol* 2015, **192**:270-278.

42. Castaño-Díez D, Al-Amoudi A, Glynn AM, Seybert A, Frangakis AS: **Fiducial-less alignment of cryo-sections**. *J Struct Biol* 2007, **159**.

43. Harapin J, Börmel M, Sapra KT, Brunner D, Kaech A, Medalia O: **Structural analysis of multicellular organisms with cryo-electron tomography**. *Nat Methods* 2015, **12**:634-636.

44. • Grant T, Grigorieff N: **Measuring the optimal exposure for single particle cryo-EM using a 2.6 Å reconstruction of rotavirus VP6**. *eLife* 2015, **4**:e06980.
Using a dose-dependent attenuation filter can improve the SNR of individual tilts and improve alignment and reconstruction results. While initially designed for SPA, this approach shows great potential for cryo-ET.

45. Chen Y, Hrabe T, Pfeffer S, Pauly O, Mateus D, Navab N, Förster F: **Detection and identification of macromolecular complexes in cryo-electron tomograms using support vector machines**. *2012 9th IEEE International Symposium on Biomedical Imaging (ISBI)*. 2012:1373-1376.

46. Wang F, Gong H, Liu G, Li M, Yan C, Xia T, Li X, Zeng J: **DeepPicker: a deep learning approach for fully automated particle picking in cryo-EM**. *J Struct Biol* 2016, **195**:325-336.

47. Chen M, Dai W, Sun SY, Jonasch D, He CY, Schmid MF, Chiu W, Ludtke SJ: **Convolutional neural networks for automated annotation of cellular cryo-electron tomograms**. *Nat Methods* 2017, **14**:983-985.

48. Castano-Diez D, Kudryashev M, Arheit M, Stahlberg H: **Dynamo: a flexible, user-friendly development tool for subtomogram averaging of cryo-EM data in high-performance computing environments**. *J Struct Biol* 2012, **178**:139-151.

49. Heumann JM, Hoenger A, Mastronarde DN: **Clustering and variance maps for cryo-electron tomography using wedge-masked differences**. *J Struct Biol* 2011, **175**:288-299.

50. Hrabe T, Chen Y, Pfeffer S, Kuhn Cuellar L, Mangold A-V, Förster F: **PyTom: a python-based toolbox for localization of macromolecules in cryo-electron tomograms and subtomogram analysis**. *J Struct Biol* 2012, **178**:177-188.

51. •• Himes BA, Zhang P: **emClarity: software for high-resolution cryo-electron tomography and subtomogram averaging**. *Nat Methods* 2018, **15**:955-961.
The hybrid approach implemented in emClarity combines 3D and 2D alignment steps by using subtomograms as fiducial markers to iteratively refine the alignment. This has resulted in a 3.1 Å structure of HIV-1 CA-SP1, representing the so far highest resolved structure in cryo-ET and subtomogram averaging.

52. Bartesaghi A, Lecumberry F, Sapiro G, Subramaniam S: **Protein secondary structure determination by constrained single-particle cryo-electron tomography**. *Structure* 2012, **20**:2003-2013.

53. Förster F, Pruggnaller S, Seybert A, Frangakis AS: **Classification of cryo-electron sub-tomograms using constrained correlation**. *J Struct Biol* 2008, **161**:276-286.

54. Chen Y, Pfeffer S, Fernández JJ, Sorzano COS, Förster F: **Autofocused 3D classification of cryoelectron subtomograms**. *Structure* 2014, **22**:1528-1537.

55. Bowden TA, Halldorsson S, Li S, Huiskonen JT, Harlos K, Li M: **Shielding and activation of a viral membrane fusion protein**. *Nat Commun* 2018, **9**:349.

56. Bharat TA, Noda T, Riches JD, Kraehling V, Kolesnikova L, Becker S, Kawaoka Y, Briggs JA: **Structural dissection of Ebola virus and its assembly determinants using cryo-electron tomography**. *Proc Natl Acad Sci U S A* 2012, **109**:4275-4280.

57. Wan W, Kolesnikova L, Clarke M, Koehler A, Noda T, Becker S, Briggs JAG: **Structure and assembly of the Ebola virus nucleocapsid**. *Nature* 2017, **551**:394-397.

58. von Appen A, Beck M: **Structure determination of the nuclear pore complex with three-dimensional cryo electron microscopy**. *J Mol Biol* 2016, **428**:2001-2010.

59. Beck M, Förster F, Ecke M, Plitzko JM, Melchior F, Gerisch G, Baumeister W, Medalia O: **Nuclear pore complex structure and dynamics revealed by cryoelectron tomography**. *Science (80-)* 2004, **306**:1387-1390.

60. von Appen A, Kosinski J, Sparks L, Ori A, DiGuilio AL, Vollmer B, Mackmull M-T, Banterle N, Parca L, Kastritis P *et al.*: **In situ structural analysis of the human nuclear pore complex**. *Nature* 2015, **526**:140-143.

61. Maimon T, Elad N, Dahan I, Medalia O: **The human nuclear pore complex as revealed by cryo-electron tomography**. *Structure* 2012, **20**:998-1006.

62. Bui KH, von Appen A, DiGuilio AL, Ori A, Sparks L, Mackmull M-T, Bock T, Hagen W, Andrés-Pons A, Glavy JS *et al.*: **Integrated structural analysis of the human nuclear pore complex scaffold**. *Cell* 2013, **155**:1233-1243.

63. Pfeffer S, Burbaum L, Unverdorben P, Pech M, Chen Y, Zimmermann R, Beckmann R, Forster F: **Structure of the native Sec61 protein-conducting channel**. *Nat Commun* 2015, **6**.

64. Brandt F, Carlson L-A, Hartl FU, Baumeister W, Grünewald K: **The three-dimensional organization of polyribosomes in intact human cells**. *Mol Cell* 2010, **39**:560-569.

65. Pfeffer S, Dudek J, Schaffer M, Ng BG, Albert S, Plitzko JM, Baumeister W, Zimmermann R, Freeze HH, Engel BD *et al.*: **Dissecting the molecular organization of the translocon-associated protein complex**. *Nat Commun* 2017, **8**:14516.

66. Braunger K, Pfeffer S, Shrimal S, Gilmore R, Berninghausen O, Mandon EC, Becker T, Förster F, Beckmann R: **Structural basis for coupling protein transport and N-glycosylation at the mammalian endoplasmic reticulum**. *Science* 2018, **360**:215-219.

67. Kudryashev M, Castaño-Díez D, Deluz C, Hassaine G, Grasso L, Graf-Meyer A, Vogel H, Stahlberg H: **The structure of the mouse serotonin 5-HT3 receptor in lipid vesicles**. *Structure* 2016, **24**:165-170.

68. Bykov YS, Schaffer M, Dodonova SO, Albert S, Plitzko JM, Baumeister W, Engel BD, Briggs JA: **The structure of the COPI coat determined within the cell**. *eLife* 2017, **6**:e32493.

69. Dodonova SO, Aderhold P, Kopp J, Ganeva I, Röhling S, Hagen WJH, Sinning I, Wieland F, Briggs JAG: **9 Å structure of the COPI coat reveals that the Arf1 GTPase occupies two contrasting molecular environments**. *eLife* 2017, **6**.

70. •• Kovtun O, Leneva N, Bykov YS, Ariotti N, Teasdale RD, Schaffer M, Engel BD, Owen DJ, Briggs JAG, Collins BM: **Structure of the membrane-assembled retromer coat determined by cryo-electron tomography**. *Nature* 2018, **561**:561-564.

This paper reports the structure of the until then structurally unknown retromer coat, combining both *in vitro* and *in situ* cryo-ET approaches. The subnanometer resolution structure of the *in vitro* assembled coat revealed a new coat architecture.

71. Briegel A, Ames P, Gumbart JC, Oikonomou CM, Parkinson JS, Jensen GJ: **The mobility of two kinase domains in the *Escherichia coli* chemoreceptor array varies with signalling state**. *Mol Microbiol* 2013, **89**:831-841.

72. Bharat TAM, Kureisaite-Ciziene D, Hardy GG, Yu EW, Devant JM, Hagen WJH, Brun YV, Briggs JAG, Löwe J: **Structure of the hexagonal surface layer on *Caulobacter crescentus* cells**. *Nat Microbiol* 2017, **2**:17059.

73. Jordan MA, Diener DR, Stepanek L, Pigino G: **The cryo-EM structure of intraflagellar transport trains reveals how dynein is inactivated to ensure unidirectional anterograde movement in cilia**. *Nat Cell Biol* 2018, **20**:1250-1255.

74. Diebolder CA, Beurskens FJ, de Jong RN, Koning RI, Strumane K, Lindorfer MA, Voorhorst M, Ugurlar D, Rosati S, Heck AJR *et al.*: **Complement is activated by IgG hexamers assembled at the cell surface**. *Science* 2014, **343**:1260-1263.

75. Albert S, Schaffer M, Beck F, Mosalaganti S, Asano S, Thomas HF, Plitzko JM, Beck M, Baumeister W, Engel BD: **Proteasomes tether to two distinct sites at the nuclear pore complex**. *Proc Natl Acad Sci U S A* 2017, **114**:13726-13731.

76. •• Guo Q, Lehmer C, Martínez-Sánchez A, Rudack T, Beck F, Hartmann H, Pérez-Berlanga M, Frottin F, Hipp MS, Hartl FU *et al.*: **In situ structure of neuronal C9orf72 poly-GA aggregates reveals proteasome recruitment**. *Cell* 2018, **172**:696-705.e12.

This study showed that 26-S proteasomes are selectively sequestered by aggregates linked to neurodegenerative diseases providing an explanation for the impaired degradation in these cells. This study is a good example of the exploratory nature of cryo-ET and subtomogram averaging when applied to cellular specimens.

77. Li X, Mooney P, Zheng S, Booth CR, Braunfeld MB, Gubbens S, Agard DA, Cheng Y: **Electron counting and beam-induced motion correction enable near-atomic-resolution single-particle cryo-EM**. *Nat Method* 2013, **10**:584-590.

78. Faini M, Prinz S, Beck R, Schorb M, Riches JD, Bacia K, Brugger B, Wieland FT, Briggs JA: **The structures of COPI-coated vesicles reveal alternate coatomer conformations and interactions**. *Science (80-)* 2012, **336**:1451-1454.

79. Dodonova SO, Diestelkoetter-Bachert P, von Appen A, Hagen WJH, Beck R, Beck M, Wieland F, Briggs JAG: **A structure of the COPI coat and the role of coat proteins in membrane vesicle assembly**. *Science (80-)* 2015, **349**:195-198.

80. Zanetti G, Prinz S, Daum S, Meister A, Schekman R, Bacia K, Briggs JA: **The structure of the COPII transport-vesicle coat assembled on membranes**. *eLife* 2013, **2**.

81. Cai S, Böck D, Pilhofer M, Gan L, Bloom KS: **The in situ structures of mono-, di-, and trinucleosomes in human heterochromatin**. *Mol Biol Cell* 2018, **29**:2450-2457.

82. Eibauer M, Pellanda M, Turgay Y, Dubrovsky A, Wild A, Medalia O: **Structure and gating of the nuclear pore complex**. *Nat Commun* 2015, **6**:7532.

83. Kosinski J, Mosalaganti S, von Appen A, Teimer R, DiGuilio AL, Wan W, Bui KH, Hagen WJH, Briggs JAG, Glavy JS *et al.*: **Molecular architecture of the inner ring scaffold of the human nuclear pore complex**. *Science* 2016, **352**:363-365.

84. Ercius P, Boese M, Duden T, Dahmen U: **Operation of TEAM i in a user environment at NCEM**. *Microsc Microanal* 2012, **18**:676-683.

85. Herzik MA, Wu M, Lander GC: **Achieving better-than-3-Å resolution by single-particle cryo-EM at 200 keV**. *Nat Methods* 2017, **14**:1075-1078.